Journal of Applied Sciences

ISSN 1812-5654

science alert

ANSInet
an open access publisher
http://ansinet.com

Journal of Applied Sciences 11 (13): 2352-2357, 2011
ISSN 1812-5654 / DOI: 10.3923/jas.2011.2352.2357

A Study on Reverse Pervaporation using Avian Eggshell as Membrane

D. Krisnaiah, W.M. Keong, M.H. Abdullah and R. Sarbatly
Chemical Engineering Program, University Malaysia Sabah,
88999 Kota Kinabalu, Sabah, Malaysia

Abstract: The development of new technologies on separation methods and applications on pervaporation has been discovered during the past decades. Based on the similar techniques, a new concept Reverse Pervaporation (RP) of gas separation into liquid has been used. The experiment was carried out by simple diffusion of free atmospheric oxygen to pure water through a prepared eggshell column which acts as natural ceramic membrane. The parameters used in this investigation are water flow rate and external pressure. Analysis on diffusion rate and influence of water flow rate and external pressure on flux performance was carried out.

Key words: Pervaporation, reverse pervaporation, gas separation, eggshell membrane

INTRODUCTION

Pervaporation, in its simplest form, is an energy efficient combination of membrane permeation and evaporation (Smitha *et al*., 2004). It's considered an attractive alternative to other separation methods for a variety of processes. Pervaporation application finds in breaking azeotropes, dehydration of solvents and other volatile organics, organic/organic separations such as ethanol or methanol removal and wastewater purification.

In pervaporation, the mass transport through a membrane is induced by maintaining permeate pressure lower than the saturated vapor pressure of the feed liquid. The driving force for permeation can be expressed in terms of the gradients of chemical potential across the membrane. Phase change of permeating species from the liquid to vapor phase is one of the distinguishing features of pervaporation (Feng and Huang, 1996a). Based on similar mechanism, reverse pervaporation concept is studied in this work where the separation of gaseous component through a membrane into liquid phase with a concentration gradient is used to allow one component in gaseous phase to preferentially permeate across the membrane. Pervaporation is typically suited to separating a minor component of a gaseous mixture, thus high selectivity through the membrane is essential.

Thus, extensive research has been performed in finding an optimized membrane material having selective interaction with a specific component of the feed mixture to maximize the performance in terms of separation factor, flux and stability. However, the performance of membranes can be largely influenced by changes in process conditions like concentration, pressure, flow rate and temperature (She and Hwang, 2004). In this perspective, an avian eggshell is chosen as a natural ceramic membrane in this study of reverse pervaporation and the effect of pressure and flow rate to mass transfer performance was carried out. Separation of atmospheric oxygen into low oxygen content pure water under different pressure and flow rate was designed in this research to determine the concept of reverse pervaporation.

MATERIALS AND METHODS

Materials: The avian eggshell used in this research is commercial hen's eggshell. Eggshell sample has density of 2.47 g cm^{-3} with calcium carbonate as active component. The sample also presented low hygroscopic moisture content (1.1%), low soluble salts content (in water) and low cation exchange capacity (9.52 meq/ 100 g). The pH of the eggshell waste sample is 8.3, which is a weak alkali. The organic matter for eggshell waste sample was found to be 5.36% which is in form of shell membranes and matrix.

Water: The water used in this experiment was normal distilled water at room temperature and pressure, with dissolved oxygen concentration less than 1 ppm (mg L^{-1}) and the experiment data was taken when the dissolved oxygen reached 1 ppm (mg L^{-1}) when flushed with nitrogen. The salinity of pure water used is zero.

Air: Room air is assumed to have normal chemical composition of 78% nitrogen, 21% oxygen, 0.9 % argon, 0.03% carbon dioxide and the remaining 0.07% is a mixture

Corresponding Author: D. Krisnaiah, Chemical Engineering Program, University Malaysia Sabah, 88999 Kota Kinabalu, Sabah, Malaysia

of hydrogen, water, ozone, neon, helium, krypton, xenon, and other trace components. Room temperature is around 18°C, with room volume approximately 231 m^3.

Material preparation

Preparation of eggshell: Six eggs with uniform colour and size were prepared. Length and width of each egg were measured and all the readings were tabulated. A 2.0 cm round iron ring are put at the top of egg and line was made by pencil following the ring shape. Then the deep scratches are made by knife following the line that has been drawn. Small hole is made at the centre of the circle and then the eggshell was chipped carefully with hand until the scratch line. This will produce a nice circular shape hole; the egg content was removed from this hole. The steps are repeated to the bottom of the egg and for each egg. Next, inside eggs are cleaned with water and protein layers were carefully removed.

Preparation of deoxygenated water: Two litre of distilled water was put into a conical flask. Nitrogen gas tank head tube was immersed into the distilled water in conical flask. Oxygen probe also immersed into the distilled water and initial reading of dissolved oxygen was taken. The control valve of nitrogen gas tank head was opened slowly to relief its gas safely and nitrogen gas was let passed through uniformly into the distilled water in the conical flask. The oxygen probe was used to measure the dissolved oxygen concentration. The control valve of nitrogen gas tank was closed when oxygen probe show the reading of dissolved oxygen concentration in distilled water are lower than 1 ppm. Then the prepared distilled water was tightly closed as fast as can before transfer to feed tank; this is to prevent oxygen from atmosphere which dissolves into the prepared distilled water.

Preparation of eggshell membrane column: The prepared eggshell was connected with each other to form a straight tube as shown in Fig. 1. A non-reactive ceramic glue was used to join the prepared eggshell. Before joining, the Teflon tape was taped around each connection to minimize the risk of cracking or leakage after gluing. The joining process was handled carefully to avoid any crack to occur in the eggshell because cracking will make water leakage to the surface during the experiment is running. The eggshell was glued into 3 pairs and let dry on flat surface. Each binding needs 2 days for it to be completely strong and stable. After that, eggshell pairs were glue to other pairs until a perfect column was produced. Notes that, this step need to ensure the joined eggshell column in straight position so that it can be insert inside Perspex tube. Next, the prepared eggshell column was tested for water leakage on surface of it by letting water passing

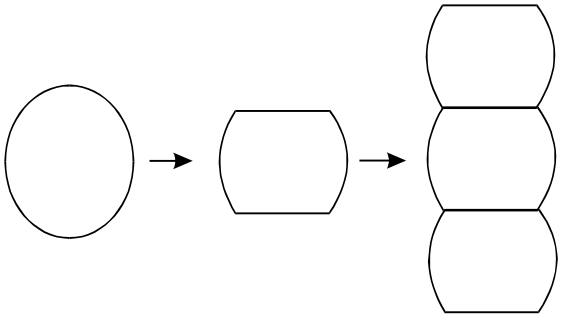

Fig. 1: Eggshell membrane column preparation

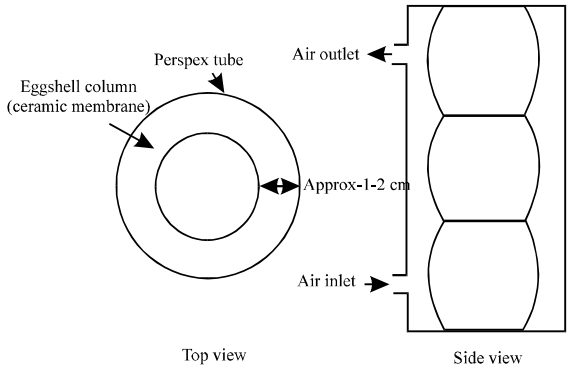

Fig. 2: Eggshell membrane column in perspe2.408×10^{-5} Tube

through it. Finally, finished eggshell column was joined using glue inside Perspex tube as shown in Fig. 2.

The experimental setup: Experimental set-up is shown in Fig. 3. It consists of a feed tank, pump, oxygen detector/probe, pressure pump, pressure regulator, water bath machine, control valve, and ceramic membrane column (egg shell). All the apparatus was connected with the long tube corresponding to required length. The oxygen probe was immersed in the water inside feed tank. Every connection was taped by Teflon tape to ensure leakage to avoid unwanted source of oxygen to dissolve into the water. The adjustable pump was used in this experiment. Pressure pump and pressure regulator was fixed to the Perspex tube. The water bath machine was used to control the temperature of deoxygenated distilled water.

The experiment procedure: The prepared distilled water was ensured less than 1 ppm (mg L^{-1}) dissolve oxygen before the experiment started. The temperature of water bath machine was adjusted to 20°C. The prepared distilled water from the feed tank was pumped into the ceramic membrane column across the control valve with flow of

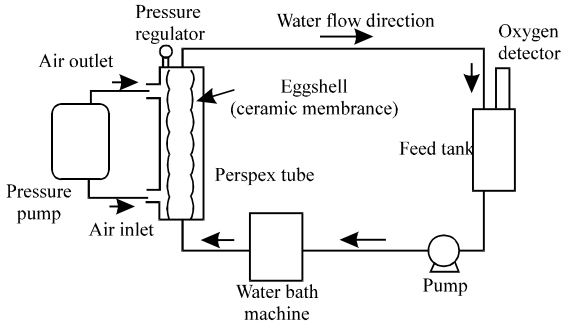

Fig. 3: The E2.408×10^{-5}periment setup

10 mL min^{-1}. The pressure pump was adjusted to 0.5 atm pressure inside the Perspex tube. The transmembrane pressure inside the Perspex tube was monitored by using two pressure gauges at both ends of the Perspex tube. Initial reading of oxygen probe was taken after the dissolved oxygen distilled water concentration reached 1ppm and the reading was taken for interval of 10 min until 100 readings. The previous steps were repeated with flow rate of distilled water of 30, 50, 80 and 100 mL min^{-1}, respectively. The experiment was repeated for pressure of 1.0, 1.5 and 2.0 atm inside the Perspex tube by adjustment on pressure pump and pressure regulator.

Data analysis

Physical properties: The length and width (thickness) of the chicken eggs were measured by a micrometer with an accuracy of 0.01 mm. The geometric mean diameter (D_g) of the chicken eggs was calculated by using the following relationships as seen in Eq. 1 (Rusu and Teodorescu, 1994):

$$D_g = (LW^2)^{1/3} \quad (1)$$

where, L is the length and W is the width (thickness) in mm.

The surface area of the chicken eggs was found by analogy with a sphere of the same geometric mean diameter:

$$S_a = \pi (D_g)^2 \quad (2)$$

where, S_a is surface area in mm^2 and D_g is geometric mean diameter in mm.

From Fig. 4, Removed surface area ≈ surface area of cone, $S_b = 2\pi rs$

Actual surface area of eggshell = S_a-S_b

Total surface area of ceramic membrane column:

$$A = (\text{no. required eggshell})\ (S_a\text{-}S_b) \quad (3)$$

Fig. 4: Appro 2.408×10^{-5} imation of removed surface area of eggshell

Pervaporation characteristics: Molecular flux is the amount of a component permeated per unit area per unit time for a given membrane.

$$J_i = \frac{Q_i}{(At)} \quad (4)$$

Where:

J_i = Flux of component i (mg min^{-1} cm^2)
Q_i = Mass of component i permeated in time
A = Effective membrane surface area (cm^2)

The flux can be plotted as a function of this measure for the driving force, which will give a better insight in the behaviour of the membrane itself.

Molecular-level interactions between membranes and diffusing species are expressed via a permeability constant used in the Arrhenius relationship:

$$P = P_{oe} - \frac{E_T}{RT} \quad (5)$$

Where:

E_p = Activation energy
P_O = Permeability constant
R = Gas constant
T = Temperature

After all data were collected, graph of oxygen concentration vs. time was plotted. Graph trend was analyzed. Flux was calculated. Then analysis of flow rate and pressure effects to flux was carried out.

RESULTS

Result and data: Table 1 shows the dimension of egg used in this experiment. The calculated value of total surface area of eggshell column, A is 398.76 cm^{-2}.

Table 2 shows calculated membrane flux at constant temperature of 20°C. Next, graph of flux against flow rate was plotted.

Analysis: At pressure 0.5 atm, flux at flow rate of 10 mL min^{-1} is relatively small, which is only

Table 1: Dimension of egg used in the experiment

Egg	Length, L (mm)	Width, W (mm)
1	57.01	44.65
2	56.93	44.50
3	57.00	44.61
4	56.96	44.59
5	56.98	44.55
6	56.90	44.60
Average	56.96	44.58

Table 2: Membrane flux at constant temperature of 20°C of different pressure and flow rate

Flux (mg cm^{-2} min^{-1})					
	Flow rate (mL min^{-1})				
Pressure (atm)	10	30	50	80	100
0.5	1.755×10^{-5}	2.408×10^{-5}	2.731×10^{-5}	3.862×10^{-5}	2.508×10^{-5}
1.0	3.950×10^{-5}	5.091×10^{-5}	5.413×10^{-5}	9.167×10^{-5}	4.915×10^{-5}
1.5	7.958×10^{-5}	1.299×10^{-4}	1.197×10^{-4}	1.521×10^{-4}	1.287×10^{-4}
2.0	9.479×10^{-4}	1.254×10^{-4}	1.633×10^{-4}	2.224×10^{-4}	1.966×10^{-4}

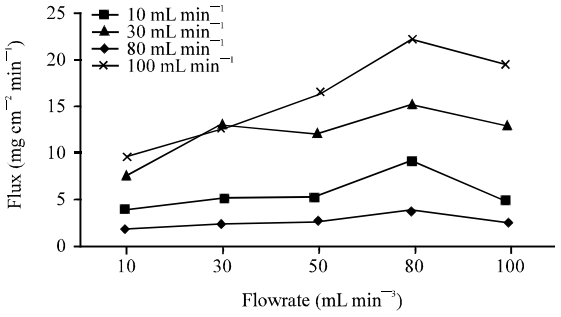

Fig. 5: Graph of flux vs. flow rate at different flow rate and pressure at constant temperature 20°C

1.755×10^{-5} mg min^{-1} cm^{-2}. As the flow rate of water increases, the flux increases until maximum flux of 3.862×10^{-5} mg min^{-1} cm^{2} was achieved at the flow rate of 80 mL min^{-1}. After that at 100 mL min^{-1} the flux decreases to 2.508×10^{-5} mg $min^{-1}cm^{-2}$.

For pressure of 1.0 atm, minimum flux was recorded at flow rate of 10 mL min^{-1}, which is 3.905×10^{-5} mg $min^{-1}cm^{-2}$. When flow rate of water increases, flux also increases. Maximum flux was achieved at flow rate of 80 mL min^{-1} which is 9.167×10^{-5} mg $min^{-1}cm^{-2}$. Then, the flux is decrease to 4.915×10^{-5} mg min^{-1} cm^{-2} at 100 mL min^{-1}. From Fig. 5, flux trend for 1.5 atm and 2.0 atm are also the same as previous pressure, where flux increasing as the flow rate increase until maximum flux is achieve at 80 mL min^{-1}, then decrease. Maximum flux for 1.5 and 2.0 atm, which achieved at 80 mL min^{-1}, was 1.521×10^{-4} mg min^{-1} cm^{-2} and 2.224×10^{-4} mg $min^{-1}cm^{-2}$, respectively.

From Fig. 6, maximum dissolved oxygen concentration achieved was around 3.9 mg L^{-1} which is 85.7% where maximum oxygen solubility in pure water at 0.5 atm and 20°C is 9.09 mg L^{-1}. The flow rate of 80 mL min^{-1} of water showed that the highest rate to achieve saturation limit of dissolved oxygen. The rate decreases follow by flow rate of 100 mL min^{-1} of water, 50 mL min^{-1} of water and 30 ml min of water. The flow rate of 10 mL min^{-1} of water showed the slowest rate to reach oxygen solubility limit at temperature of 20°C under pressure of 0.5atm.

At pressure 1.0 atm, graph showed saturation of dissolved oxygen achieved was around 8.0 mg L^{-1}. This is because increase in the pressure will increase the solubility of gases through membrane. Maximum solubility of oxygen limit from Table 2 at 20°C and 1.0 atm is 9.09 mg L^{-1}. Thus, saturation of 88% has been achieved which is higher than in pressure of 0.5 atm. Flow rate of 80 mL min^{-1} of water showed that the highest rate to achieve saturation limit of dissolved oxygen at temperature of 20°C. The rate decreases follow by flow rate of 50 mL min^{-1} of water, 30 mL min^{-1} of water, 100 mL min^{-1} of water and 10 mL min^{-1} of water showed the slowest rate to reach oxygen solubility limit at constant temperature of 20°C under pressure of 1 atm.

At pressure 1.5 atm, graph showed saturation of dissolved oxygen achieved was around 12.2 mg L^{-1} which is 89.4% of maximum solubility of oxygen (13.65 mg L^{-1}) at 20°C. From Fig. 8, the highest rate to achieve saturation limit of dissolved oxygen is flow rate of 80 mL min^{-1}. The rate decreases follow by flow rate of 100 mL min^{-1} of water, 50 mL min^{-1} of water and 30 mL min^{-1} of water. The flow rate of 10 mL min^{-1} showed the slowest rate which it take around 10 h to reach oxygen solubility limit at constant temperature of 20°C under pressure of 1.5 atm.

At pressure 2.0 atm, saturation oxygen solubility achieved was around 16.4 mg L^{-1} which is 90.2% of solubility limit, 18.19 mg L^{-1} at constant temperature of 20°C. The trend for rate of oxygen solubility at (Fig. 9) is also the same as previous pressure. Flow rate of 80 mL min^{-1} of water showed that the highest rate to achieve saturation limit of dissolved oxygen at temperature of 20°C which is 16.4 ppm. This rate decreases follow by flow rate of 100 mL min^{-1} of water, 50 mL min^{-1} of water, 30 mL min^{-1} of water. The flow rate of 10 mL min^{-1} of water showed the slowest rate to reach oxygen solubility limit at temperature of 20°C under pressure of 2.0 atm.

DISCUSSION

Effect of temperature: Water temperature has reverse effect to flux performance. Solubility of oxygen is reduced as water temperature is increase because warmer water gives more energy to oxygen molecules in the water to break free from bonding with water molecules. Therefore,

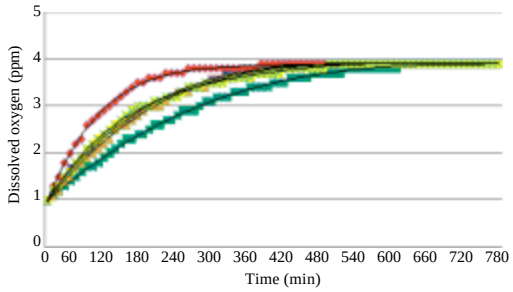

Fig. 6: Graph of dissolved oxygen vs. time at 0.5 atm and 20°C. Flow rate mL min^{-1}, ■: 10, ▲: 30, ●: 50, ◆: 80 and ×: 100

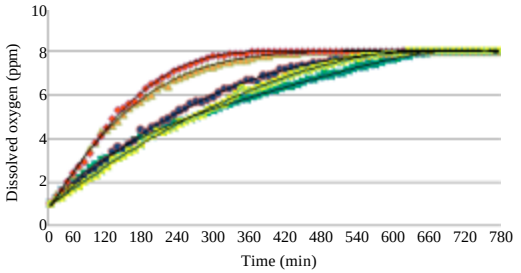

Fig. 7: Graph of dissolved oxygen vs. time at 1.0 atm and 20°C. Flow rate mL min^{-1}, ■: 10, ▲: 30, ●: 50, ◆: 80 and ×: 100

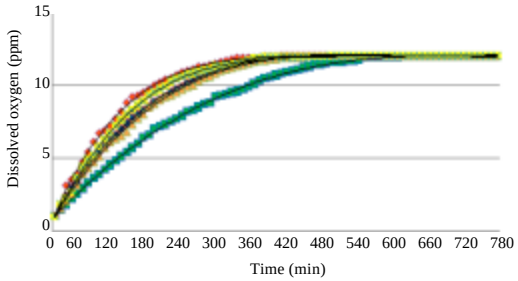

Fig. 8: Graph of dissolved oxygen vs. time at 1.5 atm and 20°C. Flow rate mL min^{-1}, ■: 10, ▲: 30, ●: 50, ◆: 80 and ×: 100

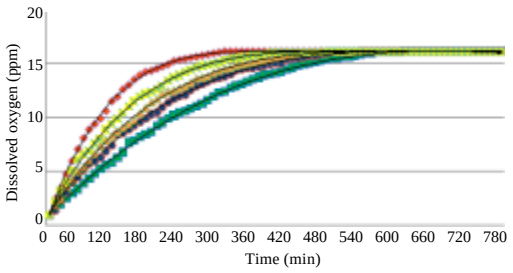

Fig. 9: Graph of dissolved oxygen vs. time at 2.0 atm and 20°C. Flow rate mL min^{-1}, ■: 10, ▲: 30, ●: 50, ◆: 80 and ×: 100

the higher water temperature will lower the diffusion rate of oxygen (Feng and Huang, 1996b). Further evidence on this point is given by the microscopic view where, unlike average pore sizes of inorganic membranes that have been reported to be constant in the temperature range 20-60°C, sizes of pores in the active layer of surface eggshell membranes can be expected to depend on operating temperature (Sharma *et al*., 2003). Changes in pore size distributions with temperature and the apparent activation energy associated with hindered transport of water and neutral solutes (oxygen) of different molecular dimensions across eggshell membrane. Therefore, by using constant temperature throughout this experiment, the effect of temperature will be assume not affect the performance of flux while studying effect of pressure and flow rate on reverse pervaporation.

On the other hand, reason of using water at constant 20°C throughout this experiment is because oxygen solubility limit at this temperature is high enough, thus any changes in dissolved oxygen concentration can easily detected. Besides that, the room temperature is around 18-23°C and it can easily maintained by using simple water bath machine.

Effect of pressure gradient: Overall values of fluxes for each flow rate under same pressure were higher than the fluxes at lower pressure in the experiment data, this was according to literature, where increases in pressure, increases the permeation of oxygen thus flux increases. It is likely that the results are due to gas component transport through defects or pinholes in the membranes which give rise to an increase in the permeance of oxygen with an increase in pressure and this factor can increase the flux proportional to any exerted pressure (Lee and Oyama, 2002). This proved that the effect of pressure gradient on the performance of mass transfer (gaseous phase component separation) via reverse pervaporation where increase in pressure, increase the flux of permeation of oxygen through membrane.

From the results, it was found that the greater permeation of oxygen through eggshell membrane by increasing pressure. The trend lines of flux (Fig. 5) at the pressure region from 0.5 to 2.0 atm was well explained by the permeation model considering the effect of pore-wall potential, while it failed to predict the optimum permeance pressure, especially under high pressures because of uncertainties of the characteristics of porous structures, such as the effects of pore-size distribution and the existence of unexpected large pin holes are always present (Yoshioka *et al*., 2001).

In fact, the contribution of concentration effect on permeation of oxygen through eggshell is less significant compare to effect of applied pressure on gaseous phase (permeate) because each run of experiment was carried out with same initial dissolved oxygen concentration in water

(1 ppm) as secondary driving force. The validity of the pressure gradient as the driving force is revealed when the conditions are changed, the values of flux vary markedly but that of concentration gradient remains essentially constant.

Effect of flow rate: For a given higher pressure of the penetrant, the flux value and dissolved oxygen limit is much greater than that of the lower pressure but the rate of reaching dissolved oxygen saturation limit is almost the same to the degree of polynomial curve on Fig. 6 to 9 at constant temperature of 20°C for each flow rate of water respectively. However, for the different flow rate of water under constant pressure and temperature, the curves lines vary greatly on degree of polynomial line. Thus, the pressure gradient clearly independent from effect of flow rate for the migration process for eggshell membrane.

According to Brown's model of random path, molecules only travelling in straight direction and changing direction by bouncing off other molecule or wall of container after collision. This can explain the reason of the diffusion flux was decreased at 100 mL min^{-1}. It is because increasing the flow rate above critical value will make water molecules to move faster and collide frequently with oxygen molecules, and make it hard for diffusion to occur thus lead to drop in flux diffusion rate considering the pore size of eggshell and oxygen molecules size. This corresponds to results presented in this preliminarily study of reverse pervaporation.

CONCLUSION

The effects of operating conditions also revealed that reverse pervaporation of low oxygen water content feed carried out at high optimum feed flow rate at relatively low temperature and high permeate external pressure was an advantage. The reason for variation in experimental outcomes of graphs may be by possible contamination of oxygen source, which each line on graphs based on their diffusivity rate to reach maximum limit solubility was affected.

ACKNOWLEDGMENT

The authors acknowledge the financial support from MOSTI, e Science grant no 03-01-10-SF0089.

REFERENCES

Feng, X. and R.Y.M. Huang, 1996a. Estimation of activation energy for permeation in pervaporation processes. J. Membrane Sci., 118: 127-131.

Feng, X. and R.Y.M. Huang, 1996b. Pervaporation with chitosan membranes. I. Separation of water from ethylene glycol by a chitosan/polysulfone composite membrane. J. Membrane Sci., 16: 67-76.

Lee, D. and S.T. Oyama, 2002. Gas permeation characteristics of a hydrogen selective supported silica membrane. J. Membrane Sci., 210: 291-306.

Rusu, M. and V.S. Teodorescu, 2004. Fractal structure of avian eggshell pores. Faculty of Physics, University of Bucharest, Romania National Institute for Material Physics, Bucharest Magurele, Romania, pp: 4.

Sharma, R.R., R. Agrawal and S. Chellam, 2003. Temperature effects on sieving characteristics of thin-film composite nanofiltration membranes: Pore size distributions and transport parameters. J. Membrane Sci., 223: 69-87.

She, M. and S.T. Hwang, 2004. Concentration of dilute flavor compounds by pervaporation: Permeate pressure effect and boundary layer resistance modeling. J. Membrane Sci., 236: 193-202.

Smitha, B., D. Suhanya, S. Sridhar and M. Ramakrishna, 2004. Separation of organic–organic mixtures by pervaporation a review. J. Membrane Sci., 241: 1-21.

Yoshioka, T., T. Tsuru and M. Asaeda, 2001. Molecular dynamics studies on gas permeation properties through microporous silica membranes. Separation Purification Technol., 25: 441-449.